Observations and Theory of High-Power Butt Coupling to $LiNbO_3$-Type Waveguides

JACOB M. HAMMER AND CLYDE C. NEIL

Abstract—We report the study and observation of high-efficiency (greater than 60 percent) and high-power (13 mW CW and 27 mW, 5 μs 5 percent duty cycle pulse) butt coupling of diode lasers to indiffused $LiNbO_3$-type waveguides. We verified the predictions of the existing coupling theory at previously unreported power levels, and present a novel theoretical explanation of the effect of multiple reflections on laser output and waveguide coupling. The theory predicts our experimental observation that the amplitude of the periodic variation of laser output with laser-waveguide separation distance is a nonmonotonic function of laser drive current.

Our measurements also lead us to infer that the onset of optical damage in Ti:$LiNbO_3$ occurs at a CW power density of 4×10^5 W/cm^2 in the 0.83 μm wavelength region.

I. Introduction

We describe the results of a program designed to study and demonstrate high-efficiency, simple butt coupling of high-power diode lasers to indiffused $LiNbO_3$ waveguides. We observed coupling efficiencies averaging well above 60 percent and a peak coupling efficiency of 73 percent. We observed the highest coupled power ever reported from diode lasers into diffused $LiNbO_3$ waveguides (13.0 mW CW and 27.6 mW for 5 μs, 5 percent duty cycle pulses). We verified the predictions of the existing coupling theory, and also developed a new theory to explain the effect of the coupling process itself on the laser output. This latter theory clarifies the mechanism causing the spatial Fabry-Perot fringes that have often been observed in butt coupling [1], [2]. In addition, we also measured a striking decrease in the incoherent power coupled into the waveguide as compared to the incoherent power leaving the laser.

We were able to obtain outstanding coupling results because of the desirable characteristics of the constricted double-heterostructure, large-optical-cavity (CDH-LOC) lasers that are produced by RCA. These lasers provide a large transverse optical cavity dimension that more closely matches the dimensions of the waveguides than the cavity of conventional diode lasers. In addition, these lasers have output powers up to 40 mW CW in a single spatial and temporal mode.

We describe the theory of the coupling process and the effect of the coupling on laser output power in Section II. Our experimental methods and procedures are described in detail in Section III. The experimental results and discussion of these results are given in Section IV, and our conclusions are presented in Section VI.

Manuscript received February 2, 1982; revised May 28, 1982. This work was supported in part by the Naval Research Laboratory under Contract N00173-80-C-0440.

The authors are with the RCA Laboratories, Princeton, NJ 08540.

A preliminary report of some of our experimental results is given in [16].

II. Theory

The theory of butt coupling between optical waveguides has been treated by many authors [3], [9]. This theory is applicable to the coupling of diode lasers to optical waveguides because the active region of a diode laser is a waveguide. The existing theory, however, does not fully treat the effect of the reflectivity of the polished-waveguide edge on the operating point of the laser. We will, therefore, present additional analysis to account for the waveguide-edge reflectivity. As will be seen, under certain conditions, even waveguide edges coated to have reflectivities as low as 1 percent can cause significant changes in laser output.

A. Coupling Efficiency

Consider the butt coupling arrangement shown in Fig. 1. Light emerging from the laser can, to a good approximation [4], be represented as having a Gaussian distribution of modal field (ϵ) in the x direction. The light is considered to be uniform in the y direction and propagates in the positive z direction. The Gaussian laser-beam waist $2\omega_L$ is measured to the points at which the maximum field ϵ_L has fallen to ϵ_L/e. The laser facet is in the x-y plane.

We make the approximation that light emerging from the waveguide (assuming that the waveguide is excited and the guided mode is traveling in the negative z direction) can also be represented as having a Gaussian distribution in the x direction. The beam waist of the waveguide mode is $2\omega_G$ measured to the $1/e$th points in field amplitude. We will assume that the polished-waveguide edge is parallel to the laser facet. With these assumptions, and for the case that the offset x_0 between the center lines of the laser and waveguide's beam waists is zero, the fractional coupling efficiency (κ) is given by [3]

$$\kappa = 2(\omega_L/\omega_G + \omega_G/\omega_L)^{-1} \left\{1 + \left[\frac{\lambda z}{\pi(\omega_L^2 + \omega_G^2)}\right]^2\right\}^{-1/2} \tag{1}$$

where z is the distance between the laser facet and the waveguide edge. The case of other than zero offset is discussed in [9] and will not be considered here. κ will be reduced if the beams are non-Gaussian. Burns [3] estimates that for the modes typical of $LiNbO_3$ guides, the actual coupling efficiency will be 0.96 κ.

In practice, the coupling efficiency is obtained by measuring the laser output at a given laser drive current when the laser

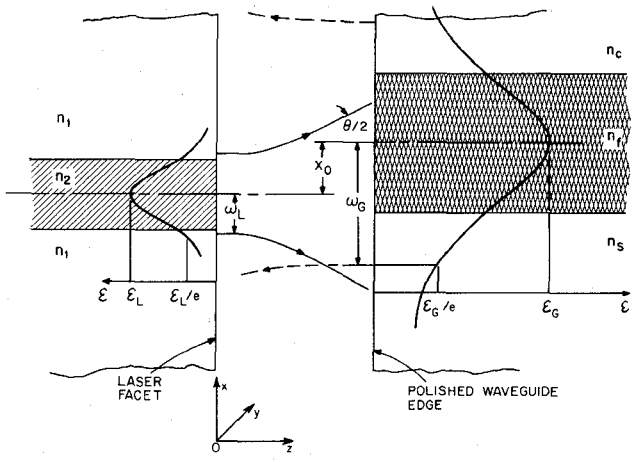

Fig. 1. Butt coupling arrangement showing definition of terms for theoretical calculation of coupling efficiency.

is remote from the waveguide. The laser is then positioned close to the waveguide as in Fig. 1, operated at the given current, and the light coupled into the waveguide is measured. The value of the coupling efficiency is then calculated assuming that the laser output at a given laser drive current is independent of the coupling process. This, as will be seen, is correct only if there is no light reflected from the waveguide back to the laser.

B. Fabry-Perot Effects

We will now consider what happens if the reflectivity of the waveguide is not zero. We first note that the objective of positioning the laser is to maximize the coupling. This results in placing the laser facet parallel and close to the optically polished waveguide edge. Two flat reflectors arranged in this way form a Fabry-Perot interferometer. (See Fig. 2.)

We picture an infinitesimally thin reflector with reflectivity equal to the waveguide-edge reflectivity R_1 combining with the reflectivity of the laser facet to form an effective laser output mirror with reflectivity R_T located at the laser output facet. In this picture, the waveguide edge is treated as having zero reflection. The coupling then is described by (1). The method of finding the output power to be used in experimentally determining the coupling is described below, and no additional correction need be applied for reflections from the waveguide edge. In this approach, we are also assuming that the external Fabry-Perot cavity formed by R_1 and R_2 does not pull the single longitudinal laser mode in any way that would affect the CW behavior [5]. This last assumption has not been experimentally tested in our present study.

The total combined reflectivity of the parallel reflectors R_2 and R_1 can readily be shown to be [6]

$$R_T = \frac{R_1 + R_2 - 2\sqrt{R_1 R_2}\cos\delta}{1 + R_1 R_2 - 2\sqrt{R_1 R_2}\cos\delta}$$

$$\delta = 4\pi Z/\lambda, \qquad \lambda = \lambda_0/n_0. \tag{2}$$

The minus sign in both the numerator and denominator is taken to account for the π phase shift in a reflection from a dielectric mirror. λ_0 is the free space wavelength and n_0 is

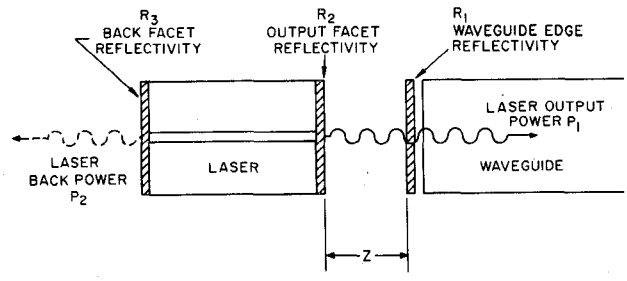

Fig. 2. Drawing defining powers and reflectivities for calculation of Fabry-Perot effect in butt coupling.

the refractive index of the medium between the laser output facet and the waveguide edge. For coupling in air, $n_0 = 1$. In (2), when $\delta = \pi, 3\pi, \cdots (2q+1)\pi$ or $z = (2q+1)\lambda/4$, q being an integer, R_T is maximized. When $\delta = 0, 2\pi, 4\pi, \cdots (2q)\pi$ or $z = (2q)\lambda/4$, R_T is minimized.

We now calculate the effect of such changes in reflectivity on the laser output power P_1 and the power coming out of the back laser facet P_2. We consider a laser with output-facet reflectivity R_T and back-facet reflectivity R_3. The total power output from both facets is P, given by the expression [7]

$$P = \frac{E_g}{e}\eta_i\left\{I - \frac{A}{\eta\beta\Gamma}\left[\Gamma\alpha_0 + \alpha_i + (2L)^{-1}\ln R^{-1}\right]\right\} \times \left(\frac{(2L)^{-1}\ln R^{-1}}{(2L)^{-1}\ln R^{-1} + \Gamma\alpha_{FC} + (1-\Gamma)\alpha_i}\right). \tag{3}$$

R is the geometric mean of R_T and R_3. $R = \sqrt{R_T R_3}$.

A is the junction area, Γ is the radiation confinement factor, and η is the laser internal efficiency at threshold. β and α_0 are material parameters, and L is the laser length (in centimeters). α_{FC} is the free carrier loss, α_i is the internal loss, and η_i is the differential quantum efficiency. E_g is the bandgap energy, e is the electronic charge, and I is the laser current.

For the CDH-LOC lasers used in the experiment reported below, the radiation confinement factor $\Gamma = 0.25$. Using the values $\alpha_0 = 215\ \text{cm}^{-1}$, $\alpha_i = 50\ \text{cm}^{-1}$, $\alpha_{FC} = 10\ \text{cm}^{-1}$ [7], we write (3) in the form

$$P = A_1\{I - A_2[104 + (2L)^{-1}\ln R^{-1}]\}\frac{2L^{-1}\ln R^{-1}}{2L^{-1}\ln R^{-1} + 40}. \tag{4}$$

For the lasers of these experiments, L is 2.5×10^{-2} cm, and thus $(2L)^{-1} = 20\ \text{cm}^{-1}$. The constants A_1 and A_2 are found by fitting (4) to the measured power-current characteristic of the laser. In these measurements, $R_T = R_2 = 0.3$ and $R_3 = 0.8$. We also use the relationship [8]

$$P_1 = \sqrt{\frac{R_3}{R_T}}\left(\frac{1-R_T}{1-R_3}\right)P_2$$

$$P = P_1 + P_2. \tag{5}$$

The CW (and long pulse) output power does not remain linear above $I = 140$ mA. We empirically adjust A_1 to match the experimental values above $I = 140$ mA. We do not, however, change the threshold current value so that A_2 remains con-

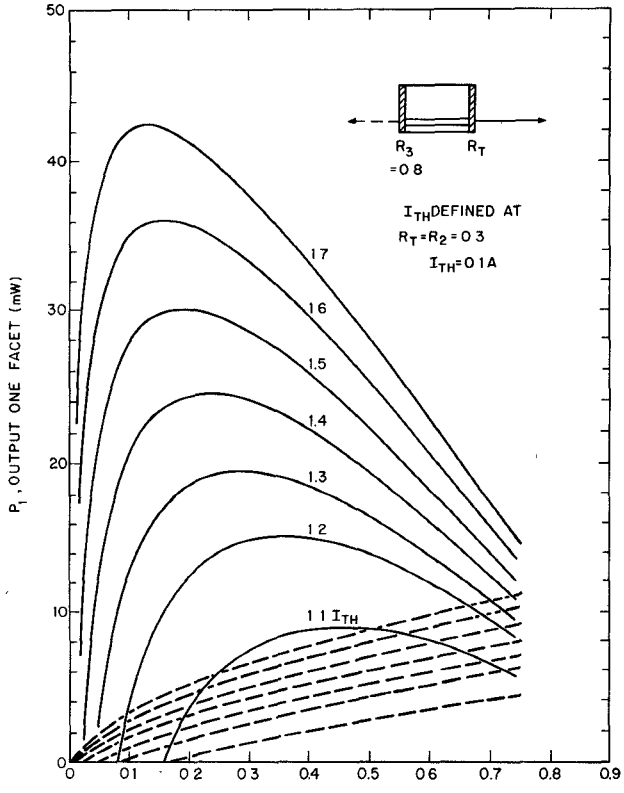

Fig. 3. Calculated single-facet output power for CDH-LOC laser a function of effective output reflectivity R_T. The parameter is the ratio of laser current to threshold current. Solid lines are output toward waveguide; dashed lines are back facet powers.

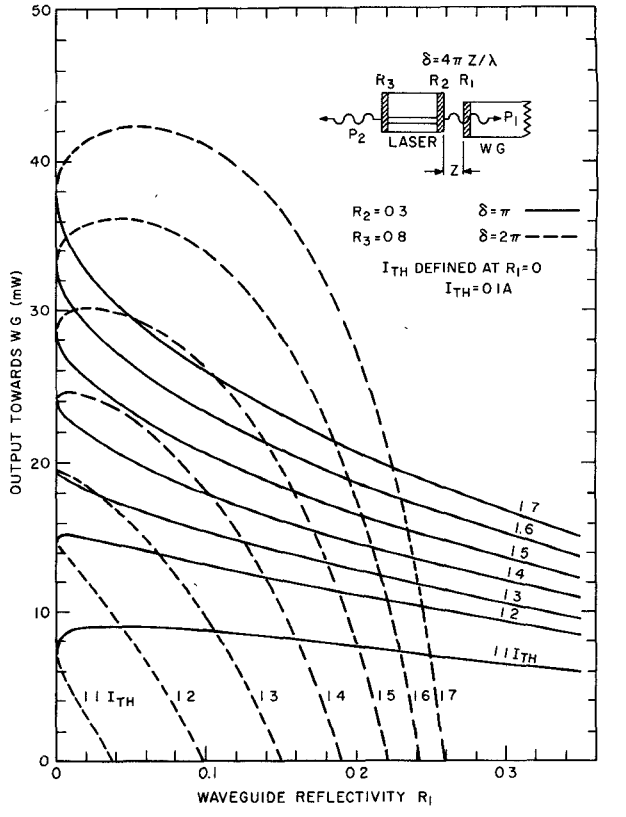

Fig. 4. Calculated CDH-LOC laser power emitted toward waveguide (P_1) as a function of waveguide reflectivity (R_1). Solid lines are for z spacing such that $\delta = 4\pi Z/\lambda = \pi, 3\pi$; dashed lines are for $\delta = 0, 2\pi, 4\pi$. The parameter is the ratio of laser current to threshold current.

stant. Fig. 3 shows plots of the output power P_1 (solid lines) and back power P_2 (dashed lines) versus R_T obtained from (4). The output-facet reflectivity R_2 is 0.3, and the back-facet reflectivity R_3 is 0.8. The parameter is the ratio of laser current to threshold current. For this laser, the threshold current (I_{TH}) is 100 mA.

We use the plots in Fig. 3 to find the actual output power during coupling. We recall that during coupling, R_T changes from a value equal to the output-facet reflectivity (R_2) to some other value described by (2), but which is unknown. Thus, both the operating point of the laser and the front-to-back power ratio change. This can be accounted for by monitoring the back-facet output P_2 and proceeding as follows.

The ratio of the change in back power between the coupled and uncoupled condition (back detector ratio) is used to multiply the value of the back power at $R_T = R_2 = 0.3$ from Fig. 3 and to find the actual value of P_2 and R_T. Using this value of R_T, a laser power correction factor is found. This is the ratio of P_1 when R_T was as above to the value of P_1 when $R_T = 0.3$. This factor is then used to multiply the direct laser output to get the correct value for use in obtaining the coupling.

We now wish to provide some additional discussion of the effect of the Fabry-Perot "fringes" described by (2) on our observations. Because R_T will have a periodic variation with z, we should observe a periodic variation in both the coupled power and in the back power. The period will be $\lambda/2$ and the spacing from maximum to minimum $\lambda/4$. Under an assumption of ideal conditions, the amplitude of the periodic variation in coupled and back-facet power may be obtained by using the value of R_T obtained from (2) in (4). We have done this for the CDH-LOC laser of this study for the extremes which occur when $\delta = \pi$ (R_T is maximized) and for $\delta = 2\pi$ (R_T is minimized). In Fig. 4, we plot the laser output (P_1) as a function of waveguide reflectivity R_1 and $\delta = \pi$ (solid lines) and for $\delta = 2\pi$ (dashed lines). The ratio of laser operating current to threshold current is the parameter. Note that in contrast to [9], even for $R_1 = 0.01$ (1 percent reflectivity), relatively large changes in laser output are predicted. At $I/I_{TH} = 1.1$, the predicted power goes from a minimum of 4.8 mW to a maximum of 8.7 mW giving a ratio (max-min)/max = 46 percent. This shift in output would occur for relative motions of $\lambda/4$ (2100 Å at $\lambda = 0.84$ μm). As the operating current is increased, the percentage change drops until a current of $1.3I_{TH}$ is reached, and it then increases more slowly as the current is further increased. What is also rather interesting is that for each value of current, a waveguide reflectivity can be found for which the change in output with z will be substantially zero. For example, at $I = 1.4I_{TH}$, this occurs at $R_1 = 0.11$ (this is the point at which the $\delta = \pi$ curve (solid line) crosses the $\delta = 2\pi$ curve (dashed line) of the same current). We thus predict that at a fixed waveguide reflectivity, the amplitude of the variations in laser output P_1, when changing z, should first decrease as the operating current increases, approach zero at some "optimum" current, and then

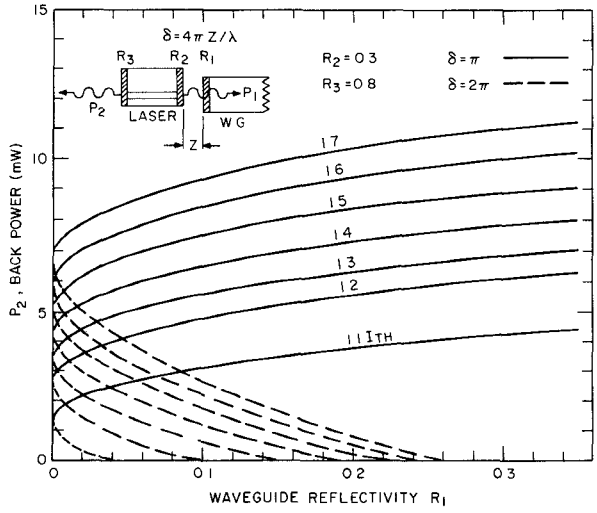

Fig. 5. Calculated CDH-LOC laser back power (P_2) as a function of waveguide reflectivity (R_1). Solid lines are for $\delta = \pi, 3\pi, 5\pi$; dashed lines are for $\delta = 0, 2\pi, 4\pi$. The parameter is the ratio of laser current to threshold current.

once again increase with further increase of operating current. This nonmonotonic variation was not predicted in the approximate treatment of Mueller *et al.* [9]. In Fig. 5, we plot the back power (P_2) as a function of waveguide reflectivity (R_1) for $\delta = \pi$ (solid lines) and for $\delta = 2\pi$ (dashed lines). The amplitude of the variations in back power with changing z should decrease slowly and monotonically as the laser current is increased.

The Fabry-Perot theory we have presented assumes perfectly parallel reflections and a parallel beam. If the laser output facet and waveguide end are tilted by some modest amount, the fringes will be less sharp and smaller, but qualitatively similar effects will be observed. There will be some effect as long as the tilt is sufficiently small so that many reflections can take place before the beam "walks off" the reflectors. We would expect that an effective waveguide reflectivity less than the actual waveguide reflectivity would suffice to represent the actual coupling as compared to the ideal case. Our theory thus predicts that the light coupled into the waveguide will show the periodic variations due to the Fabry-Perot effect (2), (4) superposed on the general drop in coupling with increasing z predicted by (1).

We might point out that the variation of laser output with the spacing of an external Fabry-Perot as described here might, in fact, be used as a convenient tool to study laser performance as a function of reflectivity.

III. Experimental Method and Procedure

A. Lasers and Optical Waveguides

The high-power and moderate-power CDH-LOC lasers used in this study are fully described in [10] and [11]. The high-power CDH-LOC laser provides CW powers of over 40 mW in a single spatial and longitudinal mode. The relatively large transverse beam waist size of these lasers allows us to obtain the high coupling efficiencies reported below.

We used Nb-diffused $LiTaO_3$ [12] (LNT) and Ti-diffused $LiNbO_3$ [13] waveguides for the coupling experiments. The LNT guide was prepared here by diffusing 600 Å of Nb into an x plate of $LiTaO_3$ for 2 h at 1180°C. The Ti-$LiNbO_3$ guide was made by Westinghouse [14]. It was formed by diffusing 280 Å of Ti into an x plate of $LiNbO_3$ for 6 h at 100°C. The orientations of the guides are shown in Fig. 6. The waveguide edges were ground and optically polished using conventional techniques. The waveguide beam waists are determined from far-field measurements.

B. Coupling

Fig. 6 is a schematic drawing of the experimental coupling arrangement. An enlarged view of the laser and mount is shown in the inset. The laser is mounted on a copper "L" mount that is grooved to accept a p-i-n detector used to monitor the light from the back laser facet. The copper "L" mount is clamped firmly to a thermoelectric cooler. A thermocouple embedded in the copper is used with a feedback circuit to the cooler to maintain constant "L" mount temperature. The laser assembly is supported in a micromanipulator with six degrees of freedom. The X-Y-Z translational motions are controlled by both "coarse" and differential micrometer screws. The differential screws can be positioned and read to 0.025 μm (250 Å).

Light butt coupled into the optical waveguide is coupled out by a $SrTiO_3$ prism. Light coupled out of the waveguide by the prism must pass through a slit to reach the calibrated p-i-n detector. The slit dimensions and position are chosen so that only the "m" line of the coupled waveguide mode [15] is allowed to pass and fall on the detector. The calibrated detector has an area of 1 cm^2 and is positioned to accept all the light passing through the slit. In this way, we ensure that all the light coupled by the prism out of the waveguide both originates in the waveguide mode and is read by the detector. The prism base is approximately 7 mm long, a length sufficient for substantially all of the guided light to be extracted.

IV. Experimental Results and Discussion

Initial coupling measurements were made using the LNT guide and a moderate-power CDH-LOC laser. Fig. 7 is a plot of coupling efficiency versus axial distance (z) for the LNT waveguide. This set of data was taken using a $LiNbO_3$ in-line output prism, and the data are corrected for the reflectivity of the output prism (14 percent) and for a measured waveguide loss of 1.65 dB in 1.5 cm. No correction for the Fabry-Perot effect was, however, taken in this measurement. The solid line is the theoretical coupling efficiency calculated from (1) using the measured values $\omega_g = 1.18$ μm and $\omega_1 = 0.47$ μm. The maximum observed value, $\kappa = 0.64$, is in reasonably good agreement with the calculated value of 0.66. The z location of the peak data point is arbitrarily set at zero. The absolute value of the spacing between the laser and the waveguide is uncertain by approximately 1.0 μm in this data set. The axial distance between data points was too large to resolve the Fabry-Perot effect in this measurement.

A similar plot of coupling efficiency versus z for early measurements on the Ti-$LiNbO_3$ waveguide is shown in Fig. 8. The coupling values are corrected for prism reflectivity and measured waveguide loss of 2.09 dB in 3.0 cm. An $SrTiO_3$

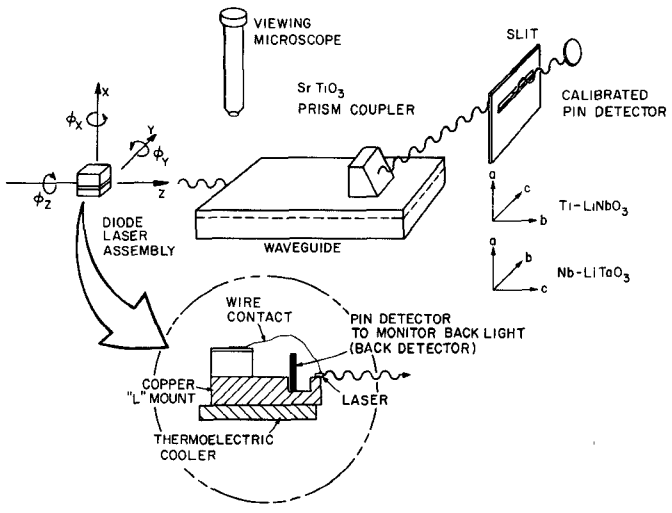

Fig. 6. Schematic drawing of experimental arrangement for measuring butt coupling.

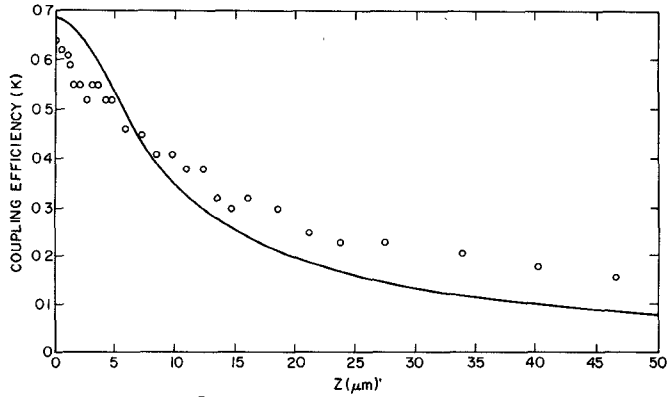

Fig. 7. Coupling efficiency of light coupled from a positive-index-guided CDH-LOC laser ($\omega_1 = 0.47$ μm) into the Nb-$LiTaO_3$ waveguide ($\omega_g = 1.18$ μm) as a function of separation distance z. The solid line is calculated from (1). The incremental steps taken in moving the waveguide are too large to resolve the Fabry-Perot effect.

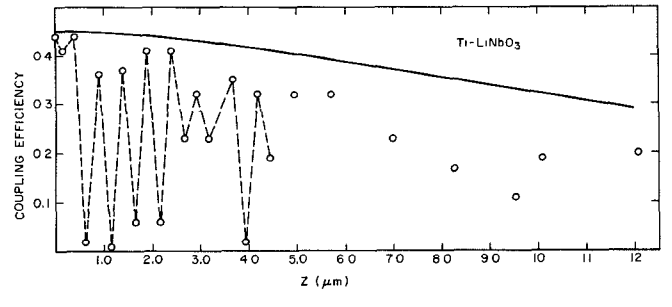

Fig. 8. Coupling efficiency of light coupled from a positive-index-guided CDH-LOC laser ($\omega_1 = 0.38$ μm) and the Ti-$LiNbO_3$ waveguide ($\omega_g = 1.62$ μm). The solid line is calculated from (1). The Fabry-Perot effect is clearly seen for $z < 4.0$ μm where finely spaced data points (connected by dashed straight-line segments) were taken.

prism output coupler was used for measurements on the Ti-$LiNbO_3$ waveguide described below. The prism had a measured reflectivity of 13 percent. A second moderate-power CDH-LOC was used. The laser-beam-transverse waist is 0.38 μm and the guide waist is 1.62 μm. The data points for z up to approximately 4.5 μm are connected to straight dashed-line segments. The Fabry-Perot effect is apparent. Closer spaced data points are, however, required for full resolution. This is done in detail for the high-power CDH-LOC laser measurements described below. The laser current is 100 mA CW or $1.04I_{TH}$, giving a laser power of 2.3 mW. The maximum power coupled into the waveguide is 1.0 mW, and the coupling efficiency is thus 0.44, which is in good agreement with the theoretical value of 0.43. The experimentally observed decrease in κ as z is increased is more rapid than the theory (1) predicts, but is obviously affected by the very strong Fabry-Perot fringes. The large amplitude Fabry-Perot fringes observed are consistent with our theory for laser operation close to threshold.

We will now describe the detailed measurements made using a high-power CDH-LOC laser. Fig. 9(a) is a power-current plot of the direct laser output (solid line) and the power coupled into the TE_0 mode of the Ti-$LiNbO_3$ waveguide (data points and dashed line). The direct laser output curve is taken for CW laser operation. There is no observable shift in this curve when the laser is operated with 5 μs, 5 percent duty cycle pulsed current. The solid circles are data points for 5 μs, 5 percent duty cycle pulses. The triangular data point is for CW operation, and represents the highest CW power, 13 mW, that we were able to couple into the waveguide. Measurements to obtain the data points above 110 mA in Fig. 9(a) were obtained by optimizing the coupling position at a single laser current (140 mA), and then proceeding to vary the laser current and take readings of the light power coupled out of the waveguide and out of the back detector. Below 110 mA, the z position was adjusted to maximize the coupling for each data point.

The threshold region is shown using enlarged scales in Fig. 9(b). A striking decrease in the amount of incoherent light coupled into the waveguide as compared to the amount directly out of the waveguide is apparent. If the coupling efficiencies were directly calculated from the data shown in Fig. 9(b), values over 100 percent would be obtained. This apparent anomaly is due to the increased effective laser reflectivity caused by the Fabry-Perot effect, resulting in increased laser output during coupling.

Table I summarizes the coupling measurements. The corrections for the Fabry-Perot effect are shown for all the measurements made with the high-power CDH-LOC laser. The early measurements made with the lower power lasers do not include the correction since we had not yet equipped these lasers with a back power detector.

For the CDH-LOC laser at high outputs, the laser power correction factors for laser currents above $1.1I_{TH}$ (110 mA) are less than 10 percent. The corrections for currents below $1.1I_{TH}$ are, as expected, larger. At $1.04I_{TH}$, the correction is over 50 percent.

The agreement between the average coupling efficiency for the 5 μs, 5 percent duty cycle data (5 μs, 5 percent) and the theoretical value is good (0.621 ± 0.060 compared to 0.69 theoretical). The discrepancy is almost within the standard deviation of the measurements. Rather small offsets (see Fig. 10) or angular misalignments could result in such discrepancies. It should be recalled that the coupling for the 5 μs, 5 percent

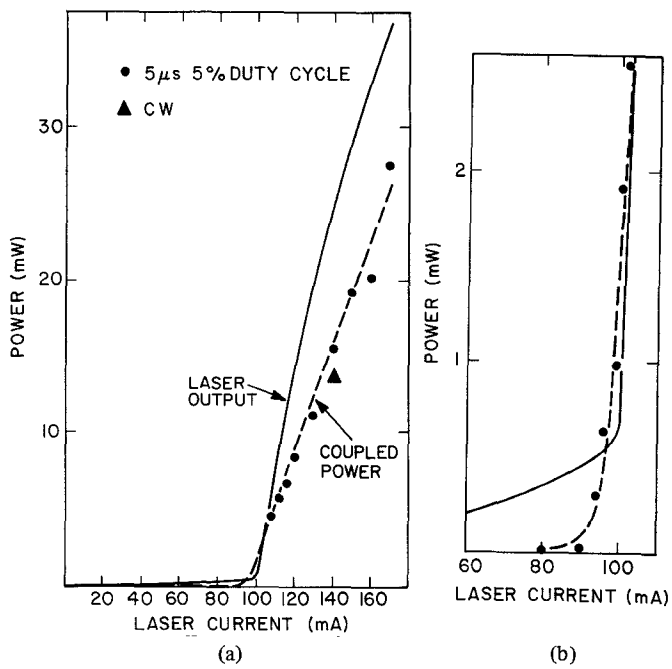

Fig. 9. (a) Light output versus current plot of high-power CDH-LOC laser in both CW and 5 μs pulse operation (solid line) and light coupled in Ti-$LiNbO_3$ waveguide mode (dashed line and data points). (b) The near threshold region shown with expanded scales.

TABLE I
SUMMARY OF EXPERIMENTAL RESULTS

CW Laser Current (mA)	Direct Laser Output (mW)	Back-Detector Ratio	Laser Power Correction Factor	Corrected Laser Power (mW)	Power Coupled into TE_0 Waveguide Mode (mW)	Coupling Efficiency Measured	Coupling Efficiency Theory
High Power CDH-LOC Laser $\omega_1 = 0.69$ μm, $\lambda = 0.839$ μm, $I_{TH} = 100$ mA; Ti-$LiNbO_3$ Waveguide $\omega_g = 1.62$ μm							κ, 0.96 κ
140 (5 μs, 5 percent Duty Cycle)	24.9	0.96	1.008	25.1	13.0	0.52	0.72, 0.69
170	36.6	0.82	1.074	39.31	27.6	0.70	
160	33.4	0.93	1.030	34.40	20.2	0.59	
150	29.2	0.96	1.007	29.40	19.3	0.66	
140	24.9	0.96	1.008	25.10	15.5	0.62	
130	19.6	1.09	0.985	19.31	11.1	0.58	
120	14.8	1.12	1.013	14.99	8.4	0.56	
116	12.2	1.10	1.021	12.46	6.7	0.54	
112	9.3	1.12	1.053	9.79	5.7	0.58	
108	6.6	1.33	1.120	7.39	4.5	0.61	
106	4.5	1.77	1.180	5.31	3.9	0.73	
104	3.2	1.44	1.526	4.88	3.2	0.66	
					5 μs, 5 percent Average	0.621 ±.060	0.72, 0.69
Moderate Power CDH-LOC Laser $\omega_1 = 0.38$ μm, $\lambda = 0.853$ μm, $I_{TH} = 96$ mA; Ti-$LiNbO_3$ Waveguide $\omega_g = 1.62$ μm							
100 mA	2.3	–	–	2.3	1.0	0.44	0.45, 0.43
Moderate Power CDH-LOC Laser $\omega_1 = 0.47$ μm, $\lambda = 0.850$ μm, $I_{TH} = 70$ mA; LNT (Nb-$LiTaO_3$) Waveguide $\omega_g = 1.18$ μm							
(46 μs, 50 percent Duty Cycle) 90 ($1.286 I_{th}$)	3.6	–	–	3.6	2.3	0.64	0.69, 0.66

data points above $I = 110$ mA was optimized only at $I = 140$ mA.

The high-power CW data point at $I = 140$ mA was independently and carefully optimized. Despite this, a coupling efficiency of only 52 percent was obtained, leading to the suspicion that some other mechanism was interfering with the coupling. We strongly suspect that optical damage to the waveguide was occurring at this CW power level. It was this

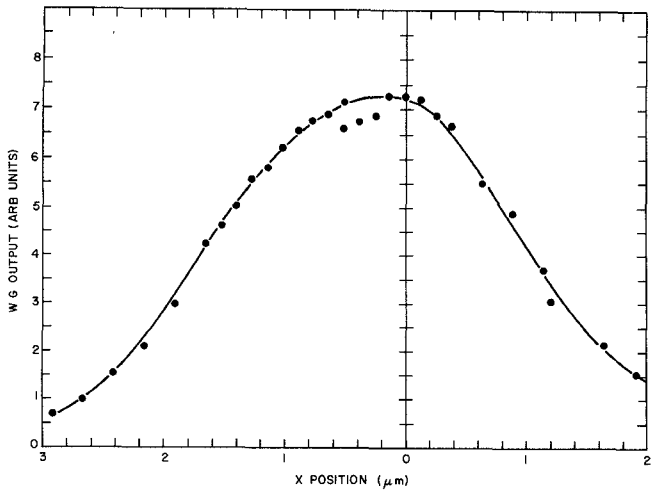

Fig. 10. Output from Ti-$LiNbO_3$ waveguide as a function of offset X. The z position is optimized at each data point.

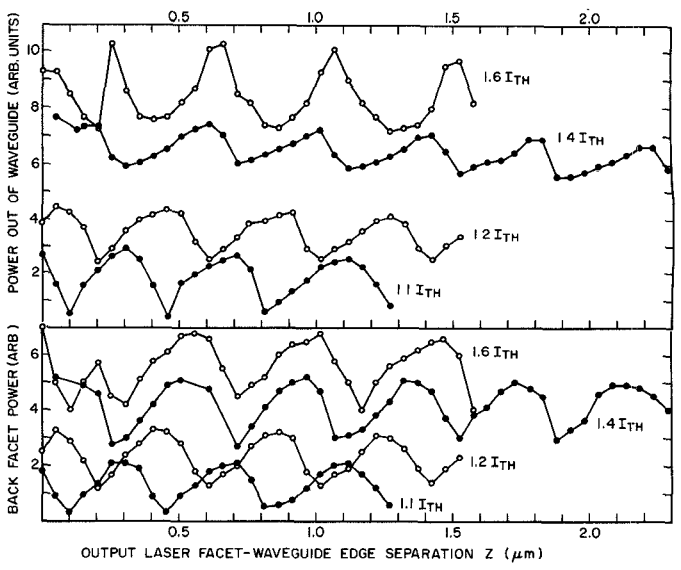

Fig. 11. Upper portion: power out of Ti-$LiNbO_3$ waveguide as a function of z with I/I_{TH} as a parameter. Lower portion: back facet power as z is varied. High-power CDH-LOC laser. The data points are connected by straight-line segments. The Fabry-Perot effect is evident.

observation that led us to favor the 5 μs, 5 percent pulse measurements which we used for all the other observations we are reporting on the coupling between the high-power CDH-LOC and the Ti-$LiNbO_3$ waveguide.

Nevertheless, the very high CW power of 13 mW coupled into the $LiNbO_3$ guide is notable. This, to the best of our knowledge, is the highest CW power coupled from a diode laser into any thin-film waveguide by any means. At this CW power level, we estimate that the optical power density is on the order of 5×10^5 W/cm^2 (CW) at the mode center, based on the measured laser lateral full beam waist of 6 μm and the full waveguide beam waist of 3.24 μm.

The variation of the light coupled out of the waveguides as a function of transverse x position (offset) is plotted in Fig. 10 for the high-power CDH-LOC-$LiNbO_3$ combination. The laser current is 140 mA, 5 μs, 5 percent pulse. The coupling is optimized by adjusting z at each data point shown. The coupling drops by 10 percent for offsets of approximately ± 0.65 μm and by 50 percent for ± 1.5 μm.

Point-by-point plots of the power coupled out of the $LiNbO_3$ waveguide as a function of z are given in the upper part of Fig. 11. The power out of the laser back facet as a function of z are given in the lower part of Fig. 11. The high-power CDH-LOC laser is used. The power scales are arbitrary. Plots for laser currents $1.6I_{TH}$ (160 mA), $1.4I_{TH}$ (140 mA), $1.2I_{TH}$ (120 mA), and $1.1I_{TH}$ (110 mA) are given. The circular data points are connected by straight-line segments. The average spacing of the data points is 0.054 μm. The periodic variation of the power with z is obvious. The average maximum-to-minimum distance (fringe spacing) is $\lambda/4$ (0.21 μm), as expected from the theory of the Fabry-Perot effect. The ratios of the maximum power to the minimum powers are given in Table II.

We thus observe that the maximum-to-minimum ratio of power coupled to the waveguide decreases with increasing current in the range $1.1I_{TH}$-$1.4I_{TH}$. The ratio then increases with increasing laser current above $1.4I_{TH}$. This behavior is predicted by the theory. As explained in Section II, the non-monotonic variation of maximum-to-minimum ratio with current follows from Fig. 4, and is in good qualitative agreement with the observation. As can be seen in Table II, the maximum-to-minimum ratio in the back facet power decreases monotonically as the laser current is increased through the entire range of observation from $1.1I_{TH}$ to $1.6I_{TH}$. This is also in good qualitative agreement with the theory, as can be verified with Fig. 5.

TABLE II
MAXIMUM-TO-MINIMUM POWER RATIOS

Laser Current	Power Out of Waveguide (Proportional P_1) Max/Min (average)	Back Facet Power Max/Min (average)
$1.1I_{TH}$	5.4	5.3
$1.2I_{TH}$	1.7	2.5
$1.4I_{TH}$	1.2	1.8
$1.6I_{TH}$	1.4	1.6

V. CONCLUSION

We have observed efficient and high-power butt coupling between diode lasers and indiffused $LiNbO_3$-type waveguides. By using a high-power CDH-LOC laser with a relatively large beam waist, we have observed coupling efficiencies as high as 73 percent and averaging 62 percent in coupling to a Ti-$LiNbO_3$ waveguide. With this laser and waveguide combination 13.0 mW (CW) and 27.6 mW (5 μs, 5 percent duty cycle pulses) optical powers have been coupled into the waveguide. These are the highest powers coupled by any means from diode lasers into $LiNbO_3$ waveguides. Our measurements also lead us to suspect that at a wavelength of 0.84 μm, optical damage occurs in $LiNbO_3$ at power densities of 5×10^5 W/cm^2 CW.

Our observations give strong support to the existing theory of butt coupling between optical waveguides. In addition, the novel theory we developed to explain the Fabry-Perot

effect that occurs during butt coupling is also substantially verified. This latter theory explains the variations that occur as a function of laser drive current and axial position. The nonmonotonic variation in the amplitude of the Fabry-Perot coupling fringes with drive current has not previously been predicted.

We observed a strong decrease in the amount of incoherent light coupled into the waveguide as compared to the amount emitted by the laser. This reduction may provide a sufficient decrease in the coupled incoherent light to satisfy the requirements of many applications using diode-laser light in $LiNbO_3$ waveguides.

Acknowledgment

We are grateful to D. Botez and J. C. Connolly for supplying the lasers used in these measurements and for many helpful discussions. We also wish to express our appreciation to M. Ettenberg for his encouragement and sound advice.

References

[1] R. G. Hunsperger, A. Yariv, and A. Lee, "Parallel end-butt coupling for optical integrated circuits," *Appl. Opt.*, vol. 16, pp. 1026-1032, Apr. 1977.

[2] D. G. Hall, J. D. Spear-Zino, H. G. Koenig, R. R. Rice, J. K. Powers, G. H. Burkhart, and P. D. Bear, "Edge coupling of a GaAlAs DH laser diode to a planar Ti:$LiNbO_3$ waveguide," *Appl. Opt.*, vol. 19, pp. 1847-1852, June 1980.

[3] W. K. Burnes, "Laser diode end-fire coupling into Ti:$LiNbO_3$ waveguides," *Appl. Opt.*, vol. 18, pp. 2536-2537, Aug. 1979. See also I. Ladany, H. J. Wolkstein, R. S. Crandall, and D. R. Patterson, "Ultra high speed modulation studies of injection lasers," Final Rep. under Contract N00173-77-C-0136, Naval Res. Lab., June 1978; and D. G. Hall, "Effects of waveguide mode asymmetry on the laser diode-to-diffused waveguide coupling efficiency," *Appl. Opt.*, vol. 18, pp. 3372-3374, Oct. 15, 1979.

[4] L. G. Cohen, "Power coupling from GaAs injection lasers into optical fibers," *Bell Syst. Tech. J.*, vol. 51, pp. 573-594, Mar. 1972; and D. Botez and M. Ettenberg, "Beamwidth approximations for the fundamental mode in symmetric double-heterojunction lasers," *IEEE J. Quantum Electron.*, vol. QE-14, pp. 827-830, Nov. 1978.

[5] C. P. Wen, J. M. Hammer, I. Gorog, F. W. Spong, and J. A. van Raalte, "Intra-cavity color selection in ion lasers," *IEEE J. Quantum Electron.*, vol. QE-2, pp. 711-713, Nov. 1966; and O. Hirota and Y. Suematsu, "Noise properties of injection lasers due to reflected waves," *IEEE J. Quantum Electron.*, vol. QE-15, pp. 142-149, Mar. 1979.

[6] M. Born and E. Wolf, *Principles of Optics*, 2nd ed. New York: Macmillan, 1964, pp. 59-66.

[7] H. Kressel and J. K. Butler, *Semiconductor Lasers and Heterojunction LED's*. New York: Academic, 1977; and D. Botez, "Optimal cavity design for low-threshold-current-density operation of double-heterojunction diode lasers," *Appl. Phys. Lett.*, vol. 35, pp. 57-59, July 1979.

[8] M. Ettenberg, H. S. Sommers, Jr., H. Kressel, and H. F. Lockwood, "Control of facet damage in GaAs laser diodes," *Appl. Phys. Lett.*, vol. 18, pp. 571-573, June 1971.

[9] C. T. Mueller, C. T. Sullivan, W.S.C. Chang, D. G. Hall, J. D. Zino, and R. R. Rice, "An analysis of the coupling of an injection laser diode to a planar $LiNbO_3$ waveguide," *IEEE J. Quantum Electron.*, vol. QE-16, pp. 363-371, Mar. 1980.

[10] D. Botez, "CW high-power single-mode operation of constricted double-heterojunction AlGaAs lasers with a large optical cavity," *Appl. Phys. Lett.*, vol. 36, pp. 190-192, Feb. 1, 1980.

[11] D. Botez and J. C. Connolly, "Single-mode positive-index guided CW constricted double-heterojunction large-optical-cavity AlGaAs lasers with low threshold-current temperature sensitivity," *Appl. Phys. Lett.*, vol. 38, pp. 658-660, May 1, 1981.

[12] J. M. Hammer and W. Phillips, "Low-loss single-mode optical waveguides and efficient high-speed modulator of $LiNb_xTa_{1-x}$ on $LiTaO_3$," *Appl. Phys. Lett.*, vol. 24, pp. 545-547, June 1974.

[13] R. V. Schmidt and I. P. Kaminow, "Metal-diffused optical waveguides in $LiNbO_3$," *Appl. Phys. Lett.*, vol. 25, pp. 458-460, Oct. 15, 1974.

[14] D. Mergerian, E. C. Malarkey, R. P. Pautienus, J. C. Bradley, G. E. Marx, L. D. Hutcheson, and A. L. Kellner, "Operational integrated optical R. F. spectrum analyzer," *Appl. Opt.*, vol. 19, pp. 3033-3034, Sept. 15, 1980.

[15] P. K. Tien, R. Ulrich, and R. J. Martin, "Modes of propagating light waves in thin deposited semiconductor films," *Appl. Phys. Lett.*, vol. 14, pp. 291-294, May 1, 1969.

[16] J. M. Hammer, D. Botez, C. C. Neil, and J. C. Connolly, "High-efficiency high-power butt coupling of single-mode diode lasers to indiffused $LiNbO_3$ optical waveguides," *Appl. Phys. Lett.*, vol. 39, pp. 943-945, Dec. 15, 1981.

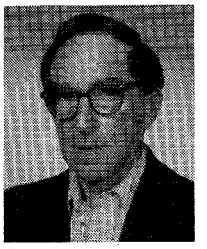

Jacob M. Hammer received the B.S. degree in engineering physics from New York University, New York, NY, in 1950, the M.S. degree in physics from the University of Illinois, Urbana, in 1951, and the Ph.D. degree in physics from New York University in 1956.

From 1956 to 1959 he worked at Bell Laboratories on microwave noise problems. In 1959 he joined RCA Laboratories, Princeton, NJ, and has worked on low-noise microwave research, electron interactions with atoms, and lasers. He spent the academic year 1968-1969 as a Senior Visitor at the Cavendish Laboratory, Cambridge, England. Since his return to RCA Laboratories in August 1969, he has been studying problems in optical communications and waveguides.

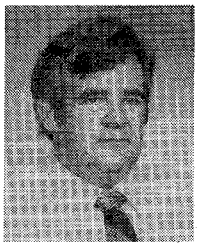

Clyde C. Neil studied electronics at Trenton Technical Institute, Trenton, NJ, and graduated in 1956. He has since taken professional advancement courses at George Washington University, Washington, DC, and Temple University, Philadelphia, PA.

He was a civilian employee of the U.S. Government from 1956 to 1959, and worked in communications systems for the Army Security Agency, Arlington, VA. He joined RCA Laboratories, Princeton, NJ, in 1959, and has worked in various areas of materials research, including chemical synthesis, low temperature studies, and optical and far infrared spectroscopy. Since 1972 he has been involved in research and development of waveguide materials, electrooptic modulators, and holographic surface gratings. He is presently working with various optical communication links and coupling junction lasers to optical fibers and waveguides.